



pubs.acs.org/estwater Article

Solving Sensor Reading Drifting Using Denoising Data Processing Algorithm (DDPA) for Long-Term Continuous and Accurate Monitoring of Ammonium in Wastewater

Xingyu Wang, Yingzheng Fan, Yuankai Huang, Jing Ling, Abby Klimowicz, Grace Pagano, and Baikun Li*



Cite This: https://dx.doi.org/10.1021/acsestwater.0c00077



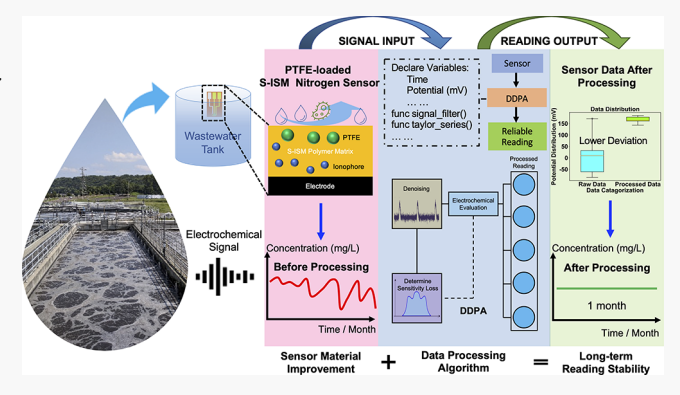
ACCESS

Metrics & More

Article Recommendations

s Supporting Information

ABSTRACT: Sensor reading drifting caused by sensor property deterioration is a major problem of long-term continuous monitoring in wastewater and hinders wide-range application of online wastewater management. This study aims to tackle this problem by developing denoising data processing algorithm (DDPA) for a typical electrochemical sensor, solid-state ion-selective membrane (S-ISM) sensor. Based on data mining and electrochemical principles, DDPA was designed by combining digital filter and outlier analysis to differentiate actual sensor readings from background noise when the S-ISM sensitivity declined over time. The sensor sensitivity was raised from 21 mV/dec to 55 mV/dec after the reading processing, without compromising the detection limit (7 \times 10 $^{-6}$ mol/L). Furthermore,



long-term accuracy of S-ISM sensors in wastewater was enhanced by adding hydrophobic polytetrafluoroethylene (PTFE) into polymer matrix. The sensitivity (57 mV/dec) of PTFE-loaded S-ISM sensors was the near-theoretical value on the first day and still higher than 35 mV/dec after 24 days in wastewater, providing an excellent stable baseline for DDPA. Combination of sensor material enhancement (adding PTFE) with sensor reading processing (using DDPA) assured the stable and high sensitivity (55 mV/dec after 24 days) and high detection limit ($<5 \times 10^{-5}$ mol/L) for wastewater monitoring. The study demonstrates a new route toward long-term accurate wastewater monitoring and smart wastewater sensor networks by establishing a strong correlation between multiorder derivatives of sensor readings and electrochemical responses with DDPA as an efficient data analysis approach.

KEYWORDS: denoising data processing algorithm, solid-state ion-selective membrane (S-ISM), wastewater, sensor reading drifting, long-term stability, data mining

1. INTRODUCTION

Water sensor network is critical for water quality monitoring, control, and management in water and wastewater treatment plants. 1,2 Electrochemical sensors have been widely used for nutrient (nitrogen and phosphorus) monitoring in wastewater on account of high selectivity, fast response, and low cost, 3,4 among which solid-contact ion selective membrane (S-ISM) sensors with open circuit potential (OCP) reading output have the appealing features of simple configuration, easy interpretation, excellent sensitivity, uncompromising rigidity, and small size. 5-12 However, S-ISM sensor property could deteriorate during long-term (e.g., days, weeks) continuous monitoring in wastewater and lead to two major problems: sensor reading drifting (sensor reading deviation from the steady status) and declined sensitivity (variation of Nernst slope over time). 13-17,17 Frequent labor-intensive and timeconsuming recalibration and maintenance (e.g., daily continuous test and monthly instantaneous test for wastewater

influent and effluent) are required to ensure the accuracy of sensor readings. Diverse sensor materials such as gold nanoparticle, ¹⁸ polymers, ^{19,20} and metal or carbon-based material including Pt, ²⁰ metal oxide₃, ²¹ graphene ²² and carbon nanotube²³ have been developed to enhance the accuracy of electrochemical sensors. However, the long-term stability of these new sensor materials is still in question, especially for wastewater containing high amounts of unknown organic/inorganic contaminants that always participate in biochemical redox reactions and cause biofouling and erosion. ²⁴ In addition, biofouling and redox reaction products inevitably

Received: July 26, 2020
Revised: December 1, 2020
Accepted: December 8, 2020



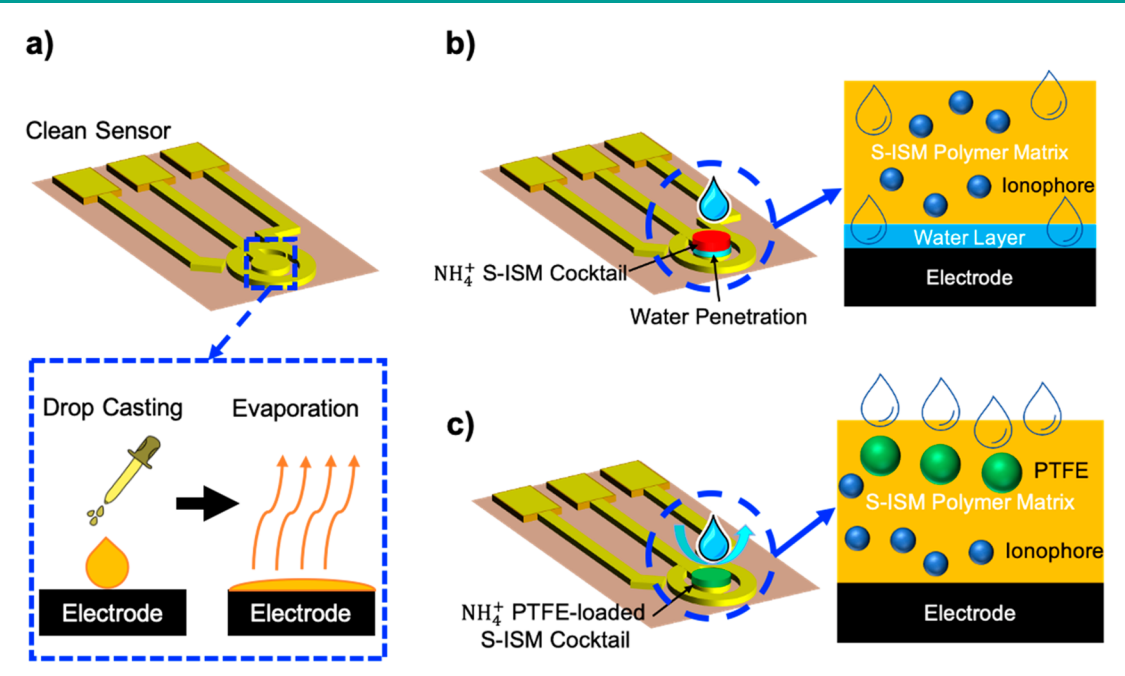


Figure 1. (a) diagram of drop-casting S-ISM polymer matrix onto the working electrode; (b) Illustration of water invasion into S-ISM sensor; (c) Illustration of water repelling from PTFE-loaded S-ISM sensor. (60–65% size).

change the adjacent environment of the sensor surface. These uncertainties makes mathematical compensation algorithm a cost-effective approach to correct sensor readings, minimize the errors generate from the sensor itself and the external environment.²⁵

Many mathematical algorithms (e.g., curve fitting²⁶) have been developed by extracting sensor features and exceptions, or embedding electrochemical models (e.g., single-analyte/ two-analyte system model²⁷) to enhance the accuracy and interpretability. Specifically, digital filters percolate anomalies from the raw data according to different signal characteristics. 17 However, the fast-declined sensitivity of electrochemical S-ISM sensors in wastewater poses difficulties for digital filters to distinguish the genuine concentration variation from sensor reading drifting. Previous studies have converted OCP signals into more sensitive amperometric current (AC) signals to alleviate the errors caused by the declined sensitivity (e.g., coulometric signal transduction). 17,28 But AC signal acquisition requires low electrode resistance, which is impossible for S-ISM sensors built upon polymer matrix. Recently, machine learning (ML) has been applied to address data drifting problem by identifying the abnormal values in actual chemical sensing communities. 29,30 But ML processes data with quite poor interpretability in a "black box" mode, and requires enormous data sets (e.g., 3 years data²⁹) to train a ML model.

S-ISM sensor, a typical electrochemical sensor capable of real-time in situ monitoring ionic contaminants (e.g., ammonium (NH $_4^+$)) in wastewater was used in this study as the sensor data source for algorithm development. The rationale for selecting ammonium as the wastewater contaminant is that it is a key factor contributing to eutrophication and dissolved oxygen (DO) depletion in water resources. SISM contains neutral or charged carrier (ionophore) to convey the ion-to-electron transduction, and produces logarithmic OCP readings with respect to the variation of target ion concentration. Since OCP only represents the resting potential between working and reference electrodes regardless

of equilibrium of reactions, it is a pure electrolytic measurement to indicate the thermodynamic stability of a system, 33,34 making it an efficient option for data processing. In this study, S-ISM sensor selectivity for ammonium (NH₄) was examined using DDPA, since NH4 is monovalent charged and has a theoretical Nernst slope of 59 mV/dec In our previous studies, S-ISM sensor demonstrated high sensitivity (53 mV/dec.), low detection limit for $NH_4^+(<5 \text{ mg/L})$, quick response (<1 s) and high selectivity ($\log K_{\mathrm{Na}^{+},\mathrm{NH}_{+}^{+}}^{\mathrm{pot}} = -2.8$ to -2.3, $\log K_{\mathrm{Ca}^{2+},\mathrm{NH}_{+}^{+}}^{\mathrm{pot}} =$ -4.8 to -3.4, $\log K_{Mg^{2+},NH_{\star}^{+}}^{pot} = -3.2$ to -4.9), 35,36 but suffered from reading drifting and short life span (less than a week in wastewater) due to the sensor material deterioration. 16,37,38 In order to prolong the sensor lifespan in wastewater, an innovative approach was explored in this study by adding superhydrophobic Polytetrafluoroethylene (PTFE)^{39,40} to the S-ISM polymer matrix⁴¹ so as to improve the hydrophobicity of S-ISM sensors and prevent water invasion into the sensor matrix.

Accurate wastewater monitoring and swift system control under various operational conditions are vital to ensure compliance with stringent water regulations and water quality management. 42,43 Despite significant progress of sensor prototypes, there has been no effective solution for real-time long-term and continuous wastewater monitoring yet due to the unreliable and drifted sensor readings caused by surface fouling, 44 short lifetime and frequent calibrations, and other environmental factors. 45 The drifting problem deteriorates sensor performance as well as spawns enormous abnormalities for various end-users (e.g., academia, 46 industries, 47 and governments⁴⁸), which poses a massive obstacle for realworld deployment of smart sensor networks. 49-51 Although latest computing technologies and specialized algorithms have been adopted and applied in gas sensors (e.g., electronic nose) to solve the drifting problem, 52 there has been little effort to conquer the limitations of general methods (e.g., regression, calibration, and ML) for S-ISM water sensors, especially for long-term continuous application in wastewater. 53 Therefore, a

reliable wastewater sensor network with customized algorithm is in urgent need to solve the sensor drifting and accomplish accurate, continuous and real-time in situ monitoring.

The objective of this study was to fundamentally solve the reading drifting of S-ISM NH₄⁺ sensors in wastewater using DDPA for long-term continuous monitoring. There were four tasks in this study. First, the association between data distribution and electrochemical response was established through the steady state test and shock test in wastewater. Different signal components from wastewater were identified and cleaned using the data distribution analysis. Second, multidimensional analysis was conducted in DDPA to display wastewater noise and improve the signal recognition through Taylor series transformation. Third, the capability of DDPA to differentiate NH₄⁺ shock from background noise was examined in wastewater by adding a series of NH₄⁺ shocks. Fourth, PTFE was added in the S-ISM polymer matrix to palliate the sensor deterioration. Long-term reading stability of the PTFEloaded S-ISM NH₄⁺ sensor was examined in wastewater for 25 days and compared with the original S-ISM NH₄⁺ sensor without PTFE. Especially, combination of sensor material enhancement (adding PTFE) with sensor reading processing (using DDPA) was explored to achieve the stable and highly sensitive NH₄ detection and ultimately improve the resilience of wastewater treatment facilities.

2. MATERIALS AND METHODS

2.1. Fabrication of Solid-State Ion Selective Membrane (S-ISM) NH₄⁺ Sensor and PTFE-loaded S-ISM NH₄⁺ Sensor. The S-ISM NH₄⁺ sensors were fabricated by drop-casting a liquid S-ISM cocktail onto the surface of a graphite working electrode (radius: 2.5 mm) on Zensor TE100 SPEs sensor (eDAQ, model ET077–40) as previously reported (Figure 1a).³⁵ 100 mg S-ISM cocktail containing ammonium ionophore, poly(vinyl chloride) (PVC) was dissolved into 500 μ L tetrahydrofuran (THF, \geq 99.5%, Sigma-Aldrich, solvent for cocktail)³⁵ and mixed ultrasonically for 5 min before drop casting on the working electrode. The sensors were then conditioned in 1 ppm of NH₄Cl solution to stabilize the S-ISM before usage.⁵⁴

For the S-ISM polymer matrix without extra protection, water can penetrate through form water layer between electrode and S-ISM (Figure 1b), and deteriorate the sensor accuracy overtime. To mitigate water invasion, S-ISM NH⁺₄ sensors were modified by adding 5% (w/w) superhydrophobic polymer, polytetrafluoroethylene (PTFE) into the aforementioned S-ISM polymer matrix. The modified sensor surface was dried under room temperature (20 °C) for 48 h. The hydrophobic PTFE-loaded sensor was expected to repel water from the electrode surface (Figure 1c) and prolong the long-term durability of sensors in wastewater.

2.2. Sensor Tests in Clean Water and Wastewater. The S-ISM $\mathrm{NH_4^+}$ sensors were first tested in the solution prepared from 100 mL deionized water and 25 $\mu\mathrm{L}$ 100 g/L $\mathrm{NH_4^+}$ standard solution. Ten pieces of S-ISM $\mathrm{NH_4^+}$ sensors made in the same batch were examined using calibration curves, through which five best performed sensors with similar and relatively constant Nernst slopes within 3 runs of calibration were selected for further tests (Supporting Information (SI) Table S1). In the steady tests, the S-ISM sensor was tested in a water solution at a constant $\mathrm{NH_4^+}$ concentration of 25 mg/L for 6 days (short-term). For the shock test, the S-ISM sensor was immersed in a water solution

(50 mL) at the initial NH $_4^+$ concentration of 16 mg/L and tested for 12 days, during which NH $_4^+$ concentration was deliberately changed by adding low (1–2 μ L)/medium (5–8 μ L)/high (15 μ L) amounts of 100 g/L NH $_4$ Cl on a random time base and adding 10 mL water on the seventh day. Successive low, medium, and high shocks were also added in the middle and at the end of test to determine the algorithm's constant performance (SI Protocol S1).

Along with clean water test, S-ISM NH₄ sensors were also tested in wastewater collected from the influent section of the UConn Wastewater Treatment Plant (WWTP) at noon time and refrigerated immediately. Average characteristics of wastewater influent are chemical oxygen demand (COD) of 300 mg/L, biological oxygen demand (BOD) of 60 mg/L, total suspended solid (TSS) of 150 mg/L and NH₄ of 15 mg/ L. S-ISM sensors were examined in wastewater for two durations: 6 days (short-term) and 25 days (long-term). In a parallel test, the PTFE-loaded S-ISM NH₄ sensor was examined in the same wastewater for 25 days (long-term). The NH₄ concentration of wastewater in the long term test beaker was verified by a commercial sensor (Professional Plus Multiparameter Instrument equipped with ammonium probe, YSI Co.) and the Nitrogen-Ammonium Salicylate TNTplus Method (HACH TNTplus 832), respectively. Specifically, the salicylate TNTplus Method was used to test the fresh wastewater collected from the UConn WWTP and couple times during the long-term test as benchmarks (SI Protocol S2), whereas the commercial sensor was used to test wastewater frequently (once per 2-3 days) throughout the long-term test (SI Protocol S3). All the tests were conducted under room temperature. The open circuit potential (OCP) readings of the original S-ISM NH₄ sensor and PTFE-loaded S-ISM NH₄ sensor were recorded using a multichannel CHI660 electrochemical potentiostat every 5 s. To determine the variation of sensor sensitivity (mV/dec.) over the test period, calibration was conducted using a series of standard NH₄ solutions (concentration: 1-64 mg/L) for both S-ISM sensor and PTFE-loaded sensor on the 1st, 5th, 10th, 15th, 20th, and 25th day.

2.3. Algorithm Structure. Outlier analysis theory was adopted in this study to develop denoising data processing algorithm (DDPA) combining with Taylor series expansion. There are three components in DDPA: Extreme value analysis and signal filtering, Density-based method on data distribution, and electrochemical evaluation (SI Figure S1). In brief, Taylor series expansion decomposes the signal corresponding function as a sum of derivative terms and reconstructs the function with limited samples and signal filters⁵⁵ so as to determine background noise and slight data drifting and subsequently eliminate it by median filter⁵⁶ (SI Figure S1a), Density-based methods reveals the distribution of sensor responses (e.g., S-ISM sensors) and Taylor series items (derivatives) from different mechanisms with histogram and kernel density estimation (KDE) to recognize sensor reading drifting caused by sensitivity declination (SI Figure S1b). The processed sensor readings (e.g., OCP data) are converted to concentration (mg/L) and evaluated using calibration curve (SI Figure S1c). Innovatively, external noise and electrochemical responses are first separated into different terms of Taylor series to prevent interference during analysis, and the abnormal drifted data generated from declined sensitivity is subsequently recognized from the changing probability density and ultimately eliminated. Here we assume that the partition

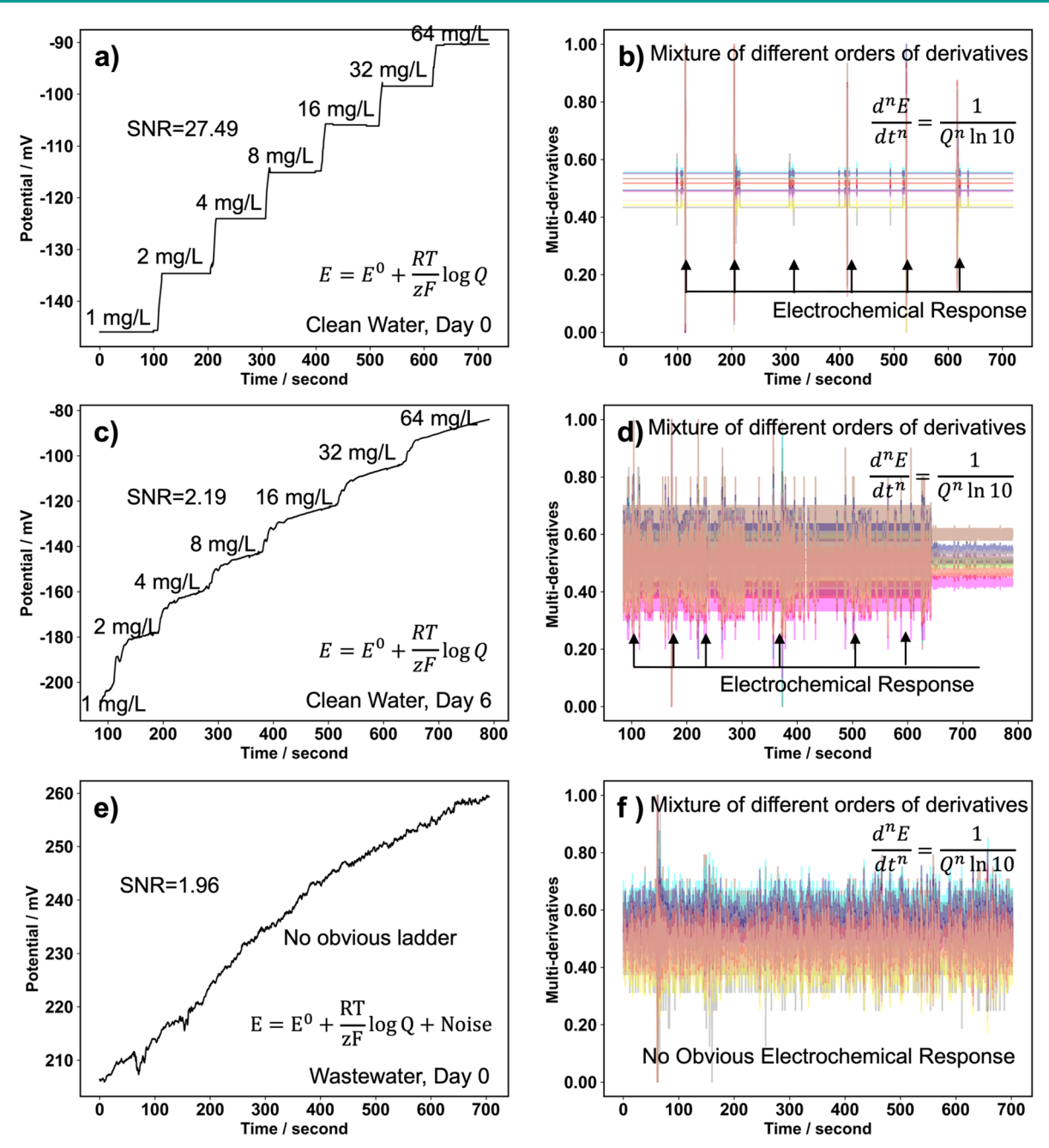


Figure 2. Illustration of the original OCP readings of S-ISM NH_4^+ sensors (a)(c)(e), scaling plot from 1st to10th of its derivatives (b)(d)(f). (Note: (a) and(b) are fresh S-ISM NH_4^+ sensor in clean water on day 0; (d) and (e) are for deteriorated S-ISM NH_4^+ sensors in clean water on day 6; and (g) and (h) are for fresh S-ISM NH_4^+ sensor in wastewater on day 0.

coefficient and mobility of the target ion at the interface between S-ISM sensor and water is always constant. 57,58

2.4. Data Collection and Analysis Using DDPA. The detailed processing steps, tools and data set of OCP reading are summarized in SI Figure S2, and the pseudo code and implementation location for the core algorithm is listed in SI Algorithm S1. Specifically, extreme analysis and signal filtering were conducted based on Taylor series expansion. Compared with Fourier Transform, Taylor series expansion avoids

resolution problem in the time domain. Although an ideal electrochemical response follows the Nernst equation, more complicated OCP patterns could occur due to complex wastewater environment. These patterns could be predicted by estimating the electrochemical response function f(t) based on limited discrete sample points. In this study, the Lagrange interpolating polynomial was deployed for the approximation of OCP-related sensor response⁵⁹ (eq 1):

$$f(t) = \sum_{i=0}^{n} f(t)L_{i}(t) + \frac{f^{(n+1)}(\xi)}{(n+1)!} \prod_{i=0}^{n} (t-t_{i}), \, \xi \in (\min(x_{0}, x_{1}, \dots, x_{n}), \, \max(x_{0}, x_{1}, \dots, x_{n}))$$

$$\tag{1}$$

in which n represent order of differentiation with upper limit of 10 in this study, and t is time. $L_i(t)$ is Lagrange polynomial representing a Kronecker delta (eq 2):

$$L_{i}(t) = \prod_{m \neq j} \frac{x_{i} - x_{m}}{x_{j} - x_{m}} = \delta_{ij} = \begin{cases} 0 \text{ if } i = j \\ 1 \text{ if } i \neq j \end{cases}$$
(2)

The last term in eq 1: $\frac{\mathbf{f}^{(n+1)}(\xi)}{(n+1)!}\prod_{i=0}^n (t-t_i)$ represents the interpolation error. The first derivative calculated from eq 1 was expressed in eq 3 and the rest derivatives can be further approximated.

$$f'(t) = \sum_{i=0}^{n} f(t) L'_{i}(t) + \frac{f^{(n+1)}(\xi)}{(n+1)!} \prod_{i=0}^{n} (t - t_{i})$$
(3)

The original data set and approximated derivatives properties were analyzed through the density-based method. The distribution of these data is expressed as a distance-based probability density entropy (eq 4):

$$E = -\sum_{i}^{m} [p_{i} \log(p_{i}) + (1 - p_{i}) \log(1 - p_{i})]$$
(4)

in which m is number of subset of features, p is probability density. A qualitative identifier enables differentiating different clusters. In this study, three subsets of features were distinguished based on the sensor behaviors in wastewater: concentration variation, data drifting, and background noise. Specifically, with the probability density increasing, data start clustering together and the value of entropy declines, and vice versa. The calculation of probability density was simplified as the distance of data points. The validation of outlier analysis between electrochemical response and declined sensitivity was quantified by Silhouette coefficient S (eq 5):

$$S_{i} = \frac{D_{\min} - D_{\text{average}}}{\max(D_{\min}, D_{\text{average}})}, (-1 < S_{i} < 1)$$
(5)

in which D_{\min} is minimum distance between two data points, D_{average} is the average distance. A high Silhouette coefficient (S>0) indicates that the data is mainly generated from electrochemical response to the concentration in water, while a low Silhouette coefficient (S<0) indicates the data is an outlier due to declined sensitivity.

3. RESULTS AND DISCUSSION

3.1. Differentiation of Sensor Reading Data Drifting and Background Noise in Clean Water and Wastewater Using Denoising Data Processing Algorithm (DDPA). S-ISM NH₄⁺ sensor was first examined in clean water with consecutive ammonium (NH₄⁺) concentrations (1–64 mg/L) on day 0. The genuine sensor readings clearly distinguished from the drifted data, presented by the short and transient "ladder" pattern due to the potential amplitude leap (Figure 2a). OCP signal is a set of sample points E_k (k is index of data) obeying Nernst equation ($E = E^0 + \frac{RT}{zF} \log Q$). The recovery of the stable electrochemical response without data drifting and background noise is a reconstruction process of the continuous function of OCP signal. Reconstruction process requires computation of weighted average of samples, 62 which is described in eq 6,

$$E(t) = \sum E_{k} \cdot w \left(\frac{t}{T} - k \right) \tag{6}$$

Where $w\left(\frac{t}{T}-k\right)$ denotes the weight function. The reconstructed function in the form of Taylor series was expressed as a sum of centered differencing formula,⁶³ described in eq 7.

$$E^{w}(t) = \sum_{n=0}^{N} a_n(t) \cdot E^n(t)$$
(7)

where a_n^w (t) is a simplified coefficient of time interval, and $E^n(t)$ is the nth order derivative. This simplified function (eq 7) expressed the electrochemical response as a sum of multiorder derivatives. As a major contributor, concentration variation could be also clearly recognized from multiorder derivatives in clean water (Figure 2b). All derivative values in Taylor series were normalized through Min–Max Feature Scaling for easy comparison. Additionally, derivatives of stable signal presented a markedly regular and clear pattern with outstanding electrochemical response without drifting or noise (SI Figure S3a), implying that DDPA is not needed to process signals from good fresh sensors in clean water.

After immersed in water solution for 6 days, the reading drifting became noticeably displayed in calibration (Figure 2c) and multiorder derivative (Figure 2d). Due to the logarithmic property of Nernst equation, the electrochemical response value exhibited clearly in the first order derivative and diminished exponentially in the higher order derivatives ($\frac{1}{Q^n \ln 10}$, Q: activity partition coefficient and related to target ion concentration; n: order), so that the 10th order derivative plot distorted much more severely than the first order derivative (SI Figure S3b). The concentration variation with high signal amplitude coincided with low amplitude data drifting in the first order derivative of the signal, while the background noise stood out in 10th order derivatives and exacerbated the electrochemical readings.

On the day 0 in wastewater doped with different concentrations of ammonium (NH₄), high-intensity interference from background noise in wastewater distorted the S-ISM sensor readings and made the concentration variation unrecognized (Figure 2e). Compared with clean water (Figure 2b), the multiorder derivatives of Taylor series in wastewater undoubtedly showed no obvious electrochemical response (Figure 2f). Nonetheless, the first order derivative still differentiated the sensor response from noise, even though it was not as obvious as that in clean water (SI Figure S3c). The 10th order derivative of the OCP signal in wastewater severely altered, and thus exhibited a completely random pattern due to the overlap with background noise. Subsequently, the noise present in higher derivatives was discarded and replenished to increase the signal-to-noise ratio (SNR, calculated by $\frac{\mu^2}{2}$) from 1.96 to 2.11. Taylor expansion provides a new mathematical perspective to differentiate clean water and wastewater, from which the first order component pattern dominated from low to high derivatives in clean water (SI Figure S3a), while the pattern in the first order derivative was completely deformed by interference even the sensor was immersed in wastewater on day 0 (SI Figure S3c).

3.2. Correction of the Declined Sensitivity of S-ISM Sensors Using Density-Based Method in 6-Day Waste-

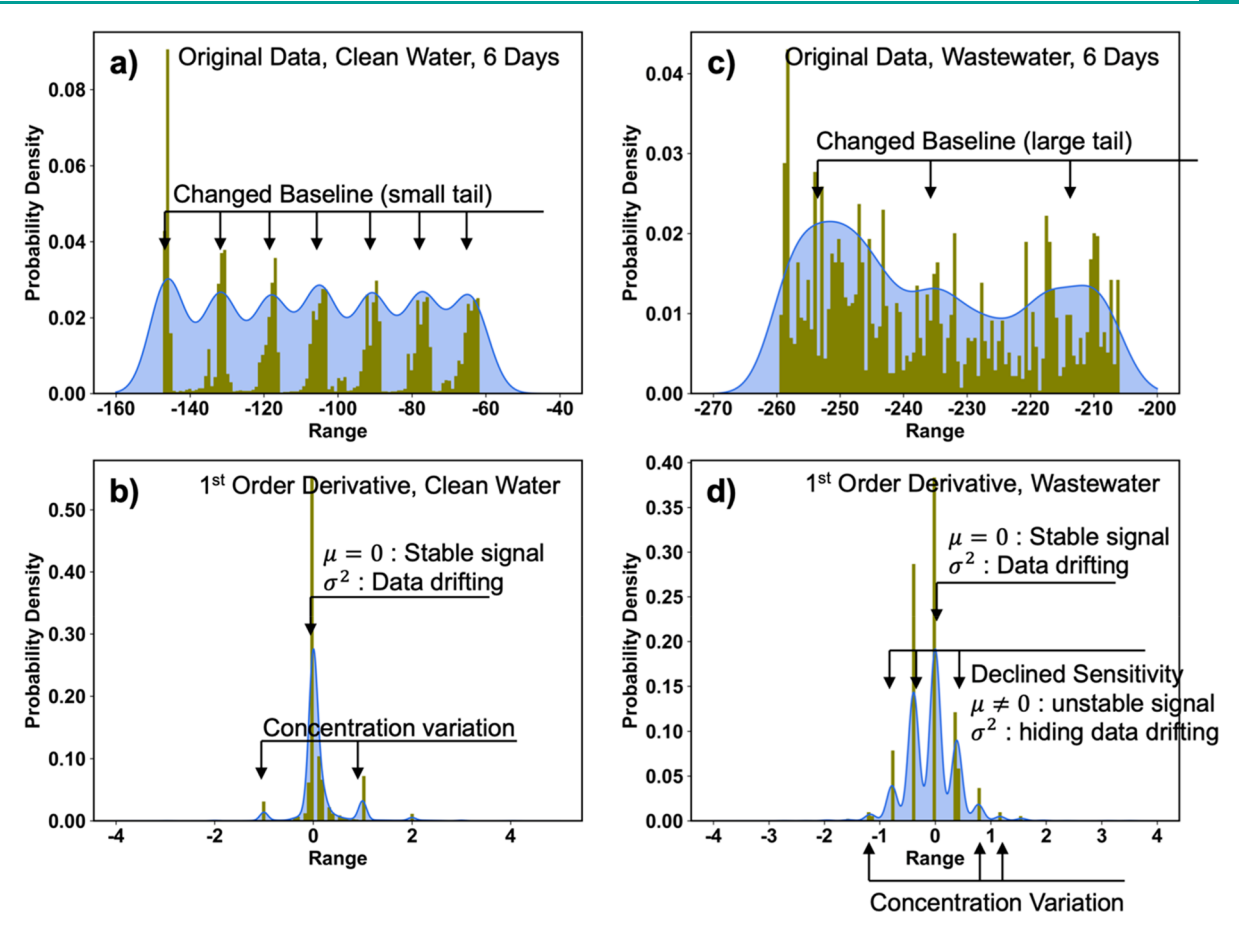


Figure 3. Histogram and kernel density estimation on sensor readings obtained in the 6-day test in clean water ((a) Original data distribution of S-ISM sensor; (b) First order derivative distribution of original data) and the 6-day test in wastewater ((c) Original data distribution of S-ISM sensor; (d) First order derivative distribution of original data).

water Test. Sensitivity declination mainly influences the sensor response to the target ion and often occurs in the long term monitoring due to sensor aging, and ultimately leads to the decrement of the Nernst slope. Taylor series expansion differentiated the concentration variation and data drifting in the first order derivative using different amplitudes with relatively stable sensitivity in clean water (SI Figure S3a). However, the amplitude between the concentration variation and data drifting became obscured in wastewater with unstable sensitivity (SI Figure S3c). The concentration variation is governed by the Nernst slope $(\frac{RT}{zF})$, but its coefficient $(\frac{1}{Q'' \ln 10})$ was canceled out in the higher order derivative. Therefore, the declined Nernst slope only reduced the amplitude of concentration variation rather than data drifting, hence exhibiting an indistinguishable mixing state overall (Figure 2d). Density-based methods was used to tackle this problem. Specifically, the histogram represents distribution of data set, while KDE infers probability density using kernel function 64 as statistics reference (eq 8):65,66

$$KDE = \frac{1}{nh} \sum_{i=1}^{n} K\left(\frac{x - x_i}{h}\right)$$
 (8)

in which n is amount of data, K is Gaussian probability density function, x is data point, and h is scaling parameter.

Through the 6-day test in clean water with different NH₄⁺ concentrations, S-ISM sensor readings exhibited a stable pattern, and each concentration formed one single bell-shaped

peak in KDE of the OCP data histogram (Figure 3a). Without concentration variation, the signal forms a Gaussian distribution peak centered at 0 as stable OCP ($\mu = 0$) and variance σ^2 as data drifting (Figure 3b). Concentration variation is transient and high amplitude, yet only consists of small part and appears separately from the huge peak on both sides in the KDE (Figure 3b).

In contrast, the KDE analysis yielded different results for the 6-day test in wastewater. Sensitivity declination caused severe sensor reading drifting and enormously fluctuated the baseline of the OCP values. Particularly, sensor reading drifting increased the variance σ^2 and led to a fat-tail distribution with a large kurtosis, meaning a dispersed data distribution and a larger deviation of data set⁶⁷ (Figure 3c). The overlapped "fat-tail" covered the peaks of concentration variation, contributing to its unobvious boundary with data drifting. For its first order derivative (Figure 3d), besides a huge peak in the middle and two small peaks on both sides, several more peaks appeared in between, indicating the baselines changed due to a declined sensitivity. Centers of these peaks (μ') are not 0 and thus caused distortion of stable signals. The "fat-tail" original data were processed with median filter excelling at signal processing for the large tail of probability density and declined sensitivity.68

As a supplement of Taylor series expansion, density-based method expresses the unobvious difference between concentration variation and hiding data drifting in the form of probability density estimation. Similar method, such as Kalman

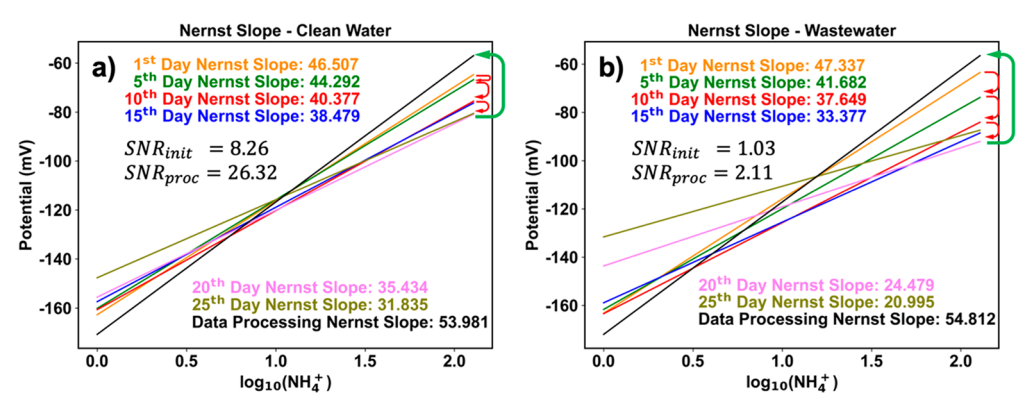


Figure 4. Calibration curve for the S-ISM sensor on the 1st, 5th, 10th, 15th, 20th, and 25th day in clean water (a) and wastewater (b). (Arrows indicate the data processing steps. Black line is the selectivity (mV/dec.) after data processing).

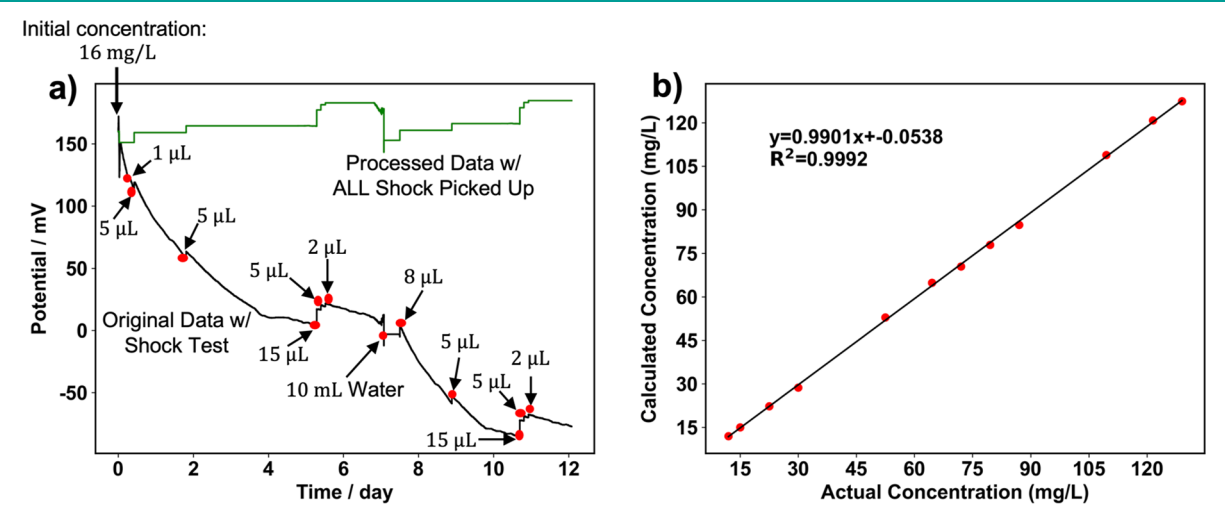


Figure 5. (a) S-ISM sensor raw readings and the processed readings (green) in the 12-day shock test in clean water; and (b) linearity correlation between the actual shock concentration and calculated shock concentration using of denoising algorithm.

filter had been found effective for detection and compensation of data drifting in sensor response.^{69–71} However, it works recursively and only provides merely the last "best estimation" without considering the whole process so that it can easily be affected by the varying sensitivity.²⁷

Elimination of sensor reading drifting is essentially related to a compensation of electrochemical response of S-ISM sensors, and thus resulting in an increase of signal-to-noise ratio (SNR = $\frac{\mu}{\sigma^2}$), square ratio of average and standard deviation for the normalized data set). When background noise and reading drifting are recognized and eliminated through DDPA, the SNR value rises and the sensor readings demonstrate higher sensitivity, reflected by the improvement of the Nernst slope. Based on standard thermodynamics, the theoretical value of Nernst slope should be 59 mV for NH₄. When S-ISM sensors are immersed in wastewater over time, water invasion into the S-ISM polymer matrix and fouling on the S-ISM surface reduce the sensor response (SI Figure S4), and ultimately lead to the declined Nernst slope (red arrows in Figure 4). The Nernst slope of the S-ISM sensor dropped mildly within 25 days in clean water (46-32 mV/dec., Figure 4a), while it dropped drastically within 25 days in wastewater (47-21 mV/dec., Figure 4b), and ultimately led to the sensor reading undetectable. With data drifting and background noise being removed from the sensor reading, the proportion of the actual OCP signals increased, leading to an enhanced signal quality

(green arrows in Figure 4) and corrected Nernst slope (55 mV/dec., black line in Figure 4b) closer to the ideal value (59 mV/dec.).

Compared with other methods, DDPA was specifically developed to fit S-ISM sensors by overcoming the limitations of general-purpose-based algorithms, such as oversimplification of wastewater (Generic algorithm, GA⁷²), noise interference (fast fixed-point algorithm, fastICA⁷³), huge training data set, and false data deterioration (artificial neural network, ANN, response processing, CRP⁷⁵). Furthermore, DDPA is the only method capable of applying to the real wastewater continuously and improve sensor sensitivity for up to 4 weeks (SI Table S2).

3.3. Quantify the Transient NH₄⁺ Shocks Using the Denoising Data Processing. The capability of DDPA to accurately restore sensor signals under transient shocks was examined using a series of NH₄⁺ shocks (low/medium/high amount) introduced in a water solution over 12-day period. Here, an S-ISM sensor with severe sensor reading drifting even under the steady state without shock was used to verify the denoising capacity of DDPA. The results showed that even under this worst-case scenario, the huge drifting (~200 mV) was completely erased and all the NH₄⁺ shocks were successfully captured by the algorithm over time (Figure 5a). The key point is that rather than original data, the DDPA applies a median filter onto the derivatives, which represents

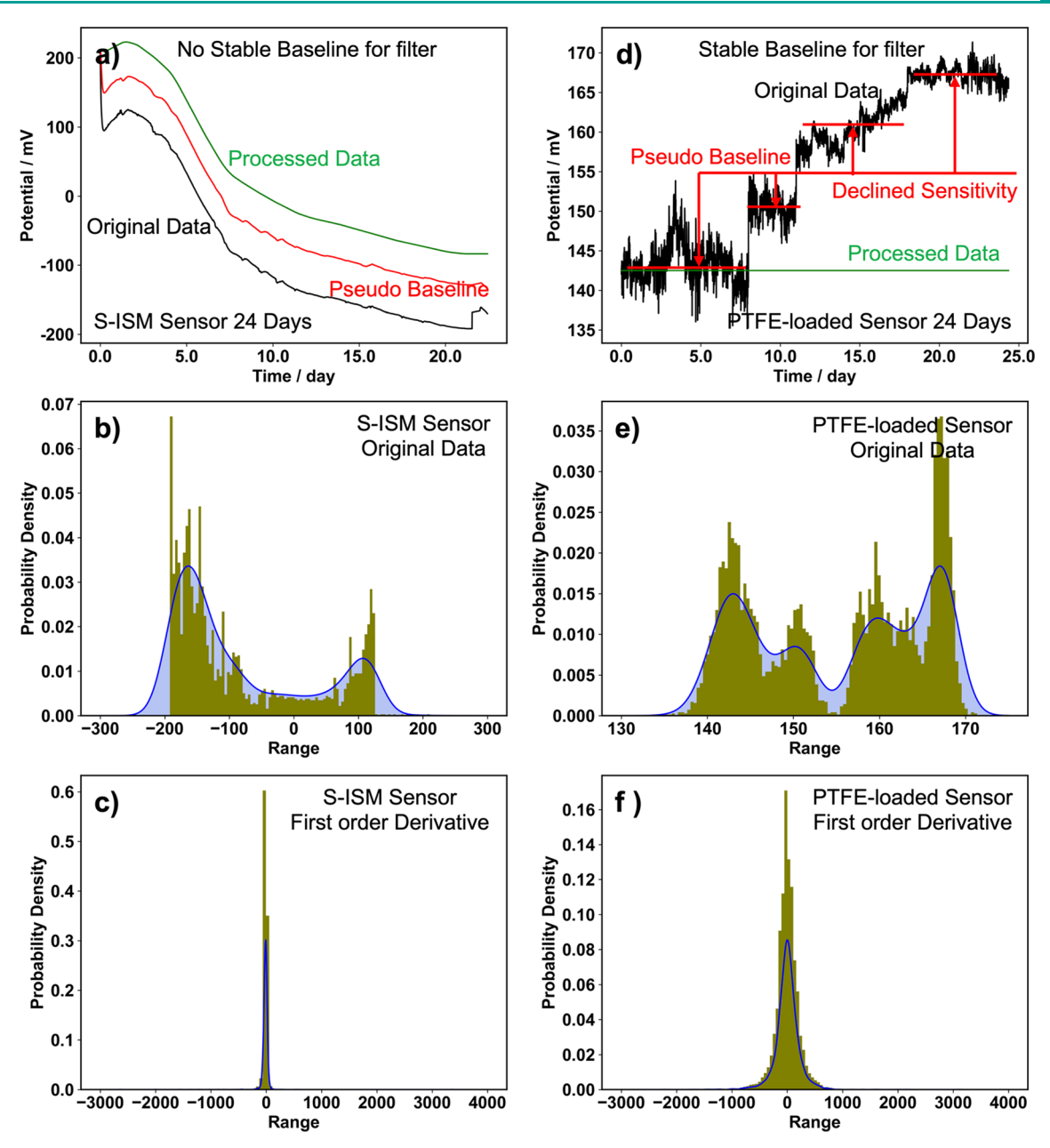


Figure 6. S-ISM sensor test in wastewater for 25 days. (a) Original and processed data of S-ISM sensor; (b) Original data distribution of S-ISM sensor; (c) First order derivative data distribution of S-ISM sensor; (d) Original and processed data of PTFE-loaded S-ISM sensor; (e) Original data distribution of PTFE-loaded S-ISM sensor; (f) First order derivative data distribution of PTFE-loaded S-ISM sensor.

the changing rate and relies upon the Nernst Equation, utterly different from background noise or drifting, so that these shocks can be differentiated in DDPA after filtration, without sacrificing the capability of determining shocks. More importantly, there is an excellent linear relationship ($R^2 = 0.9992$) of the shock concentration (X axis) and the calculated shock concentration using DDPA (Y axis) (Figure 5b), clearly demonstrating that the DDPA can accurately calculate the shock concentration variation after adjusting the data drifting without sacrificing the detection limit.

3.4. Enhanced Sensitivity of PTFE-Loaded S-ISM Sensor in 25-Day Wastewater Tests Using DDPA. S-ISM sensor readings acquired from the long-term test (25 days) in wastewater were processed using DDPA, and suffered severe data drifting (Figure 6a). The statistical analysis revealed that the original data distribution exhibits two peaks

in the KDE plot (Figure 6b), while there are no corresponding baselines to these two peaks in the processed data (Figure 6a), meaning that the sensor essentially lost accuracy and only produced unpredictable data. Therefore, signal filter cannot work and the KDE of signal derivative's probability density cannot reflect drifting accurately (Figure 6c).

In contrast, the PTFE-loaded S-ISM sensor exhibited a high sensitivity (Nernst slope) in the long term wastewater test (SI Table S3). For the original S-ISM sensor without PTFE, the declined sensor sensitivity is mainly caused by S-ISM sensor surface erosion and water penetration in between S-ISM polymer matrix and electrode (Figure 1a).³⁵ The hydrophobic PTFE protected S-ISM surface from erosion by repelling water and extended the durability of the sensor (Figure 1b), and thus solving the unpredictable reading problem of S-ISM sensors and providing a relatively stable sensitivity and baseline of the

sensor readings. However, the nitrogen concentration (mg/L) could not be accurately calculated from the conversion of the original OCP readings (mV) of PTFE-loaded sensor due to the declined sensitivity (mV/dec.) and the undetermined reading drifting (Figure 6d, gray line in SI Figure S5). This problem can be solved by DDPA. The KDE plot of the PTFE-loaded sensor possesses four peaks, corresponding to the baselines (red lines in Figure 6d) with all the data vibrating with a certain range, indicating a regular and predictable pattern. The processed reading (blue line in SI Figure S5) has a much smaller range of concentration fluctuation (<2 mg/L), which is acceptable compared with raw concentration data before processing (>10 mg/L). The median filter distinguished and eliminated data drifting and background noise from the actual OCP response by removing the deviation values in the Taylor series and then generated the stabilized OCP signal with each baseline. The KDE and histogram of first order derivatives show only one peak (Figure 6f), meaning that there was no concentration variation and the baseline variation was caused from data drifting. All the data were calibrated and finally yielded a stable reading for the PTFE-loaded S-ISM sensor in the long term wastewater test (green line in Figure 6d). Furthermore, DDPA compensated the declined sensor sensitivity (mV/dec., Nernst slope), enabling an accurate conversion from OCP readings (mV) to nitrogen concentration values (mg/L) over time (green line in SI Figure S5), which was appropriately validated by both commercial ammonium sensor (red points in SI Figure S5) and salicylate TNTplus test (pink points in SI Figure S5).

3.5. Advantages and Future Challenges. Current solutions for monitoring contaminants, 76,77 improving water sensor sensitivity and accuracy,⁷⁸ and extending sensor lifespan⁷⁹ are inadequate for long-term continuous wastewater monitoring. Commonly used ammonium sensors have limited capability of drifting adjustment (<45 mV), require frequent manual calibration, and cannot last in wastewater even for a couple hours. In contrast, the solution presented in this study can achieve continuous wastewater monitoring for 25 days and only needs the initial calibration. To compensate for the fragility of sensor materials in wastewater, a novel algorithm, DDPA was developed specifically for complex sensor reading processing, enabling dissecting the S-ISM sensors readings, removing background noise, and minimizing the bias. Furthermore, the newly developed PTFE-loaded sensor physically alleviated the unpredictable sensor readings for DDPA analysis. The combination of sensor material enhancement (adding PTFE) and data processing (using DDPA) established a "foundation-superstructure" platform defeating commercial sensor solutions to fundamentally solve sensor reading drifting and can be applied to a broad spectrum of sensors for long-term accurate and continuous monitoring in a complex water environment. Currently, DDPA mainly embedded an electrochemical Nernst equation without deep consideration of S-ISM surface fouling because the formation mechanism and kinetics are not clear yet. 80 We've noticed the fouling on the sensor surface changes mass (ions) and electron transfer between bulk water and S-ISM polymer matrix, and ultimately interferes with the sensor electrochemical response. In future studies, an electrochemical fouling/biofouling and S-ISM interaction model will be modulated and incorporated with DDPA to boost its correction capability, advance sensor accuracy, and diminish reading drifting in long-term wastewater monitoring.

ASSOCIATED CONTENT

Solution Supporting Information

The Supporting Information is available free of charge at https://pubs.acs.org/doi/10.1021/acsestwater.0c00077.

The flowchart for components and mechanisms of denoising data processing algorithm (DDPA). The flowchart of data processing steps of the algorithm, data points, and toolkits for implementation. The illustration of separate derivative plots of S-ISM NH₄ sensor readings on Day 0 in clean water, Day 6 in clean water and Day 0 in wastewater. The SEM image of sensor surface fouling after immersed in wastewater for 25 days. The 25 days calculated concentration (mV) from the PTFE-loaded S-ISM sensor reading (mV) using DDPA simulation in wastewater and validation by commercial sensor and salicylate test. The pseudo code of DDPA algorithm and the GitHub address of the Python implementation. The Nernst slope results of ten tested sensors. The comparison of DDPA and other algorithms in terms of sensitivity (mV/dec.) and detection limit (NH₄, M) improvement for electrochemical sensors. The comparison of the sensitivity of SOISM Sensor and PTFE-loaded S-ISM sensor throughout 25 days tests in wastewater. The shock test protocol. The Nitrogen-Ammonium salicylate TNTplus test protocol. The YSI commercial ammonium sensor testing protocol (PDF)

AUTHOR INFORMATION

Corresponding Author

Baikun Li — Department of Civil & Environmental Engineering, University of Connecticut, Storrs, Connecticut 06269-3037, United States; orcid.org/0000-0002-5623-5912; Phone: 860-486-2339; Email: baikun.li@uconn.edu

Authors

Xingyu Wang — Department of Civil & Environmental Engineering, University of Connecticut, Storrs, Connecticut 06269-3037, United States

Yingzheng Fan – Department of Civil & Environmental Engineering, University of Connecticut, Storrs, Connecticut 06269-3037, United States

Yuankai Huang — Department of Civil & Environmental Engineering, University of Connecticut, Storrs, Connecticut 06269-3037, United States

Jing Ling – Department of Civil & Environmental Engineering, University of Connecticut, Storrs, Connecticut 06269-3037, United States

Abby Klimowicz — Department of Civil & Environmental Engineering, University of Connecticut, Storrs, Connecticut 06269-3037, United States

Grace Pagano – Department of Civil & Environmental Engineering, University of Connecticut, Storrs, Connecticut 06269-3037, United States

Complete contact information is available at: https://pubs.acs.org/10.1021/acsestwater.0c00077

Notes

I

The authors declare no competing financial interest.

ACKNOWLEDGMENTS

This study was supported by National Science Foundation (NSF) Environmental Engineering Program GOALI Project (Grant No. 1706343), NSF Partnerships for Innovation (PFI) Accelerate Innovative Research (AIR) Project (Grant No. 1640701), Connecticut Biopipeline Program, and Connecticut SPARK Program. Xingyu Wang was partially supported by School of Engineering GE Fellowship at University of Connecticut. The project was also partially funded by Infiltrator Water Technologies LLC.

REFERENCES

- (1) Goal 6: Clean water and sanitation https://www.undp.org/content/undp/en/home/sustainable-development-goals/goal-6-clean-water-and-sanitation.html (accessed 2020/3/30).
- (2) WHO | Progress on household drinking water, sanitation and hygiene 2000–2017: http://www.who.int/water_sanitation_health/publications/jmp-report-2019/en/ (accessed 2020/3/30).
- (3) Arvand, M.; Asadollahzadeh, S. A. Ion-Selective Electrode for Aluminum Determination in Pharmaceutical Substances, Tea Leaves and Water Samples. *Talanta* **2008**, *75* (4), 1046–1054.
- (4) Zamani, H. A.; Mohammadhosseini, M.; Nekoei, M.; Ganjali, M. R. Determination of Erbium Ions in Water Samples by a PVC Membrane Erbium-Ion Selective Electrode https://www.ingentaconnect.com/content/asp/senlet/2010/00000008/00000002/art00016 (accessed 2020/4/14). DOI: 10.1166/sl.2010.1268.
- (5) Li, J.; Xia, J.; Zhang, F.; Wang, Z.; Liu, Q. An Electrochemical Sensor Based on Copper-Based Metal-Organic Frameworks-Graphene Composites for Determination of Dihydroxybenzene Isomers in Water. *Talanta* **2018**, *181*, 80–86.
- (6) Chen, K.; Zhang, Z.-L.; Liang, Y.-M.; Liu, W. A Graphene-Based Electrochemical Sensor for Rapid Determination of Phenols in Water. *Sensors* **2013**, *13* (5), 6204–6216.
- (7) Tan, F.; Cong, L.; Li, X.; Zhao, Q.; Zhao, H.; Quan, X.; Chen, J. An Electrochemical Sensor Based on Molecularly Imprinted Polypyrrole/Graphene Quantum Dots Composite for Detection of Bisphenol A in Water Samples. Sens. Actuators, B 2016, 233, 599–606.
- (8) Afkhami, A.; Soltani-Felehgari, F.; Madrakian, T.; Ghaedi, H.; Rezaeivala, M. Fabrication and Application of a New Modified Electrochemical Sensor Using Nano-Silica and a Newly Synthesized Schiff Base for Simultaneous Determination of Cd2+, Cu2+ and Hg2+ Ions in Water and Some Foodstuff Samples. *Anal. Chim. Acta* 2013, 771, 21–30.
- (9) Moraes, F. C.; Rossi, B.; Donatoni, M. C.; de Oliveira, K. T.; Pereira, E. C. Sensitive Determination of 17β -Estradiol in River Water Using a Graphene Based Electrochemical Sensor. *Anal. Chim. Acta* **2015**, *881*, 37–43.
- (10) Lindfors, T. Light Sensitivity and Potential Stability of Electrically Conducting Polymers Commonly Used in Solid Contact Ion-Selective Electrodes. *J. Solid State Electrochem.* **2009**, 13 (1), 77–89
- (11) Salem, A. A.; Barsoum, B. N.; Izake, E. L. Potentiometric Determination of Diazepam, Bromazepam and Clonazepam Using Solid Contact Ion-Selective Electrodes. *Anal. Chim. Acta* **2003**, 498 (1), 79–91.
- (12) Crespo, G. A.; Macho, S.; Bobacka, J.; Rius, F. X. Transduction Mechanism of Carbon Nanotubes in Solid-Contact Ion-Selective Electrodes. *Anal. Chem.* **2009**, *81* (2), 676–681.
- (13) Banna, M. H.; Imran, S.; Francisque, A.; Najjaran, H.; Sadiq, R.; Rodriguez, M.; Hoorfar, M. Online Drinking Water Quality Monitoring: Review on Available and Emerging Technologies. *Crit. Rev. Environ. Sci. Technol.* **2014**, *44* (12), 1370–1421.
- (14) Gupta, K. C.; Jeanne D'Arc, M. Effect of Concentration of Ion Exchanger, Plasticizer and Molecular Weight of Cyanocopolymers on Selectivity and Sensitivity of Cu(II) Ion Selective Electrodes. *Anal. Chim. Acta* **2001**, 437 (2), 199–216.

- (15) Fibbioli, M.; Bandyopadhyay, K.; Liu, S.-G.; Echegoyen, L.; Enger, O.; Diederich, F.; Bühlmann, P.; Pretsch, E. Redox-Active Self-Assembled Monolayers as Novel Solid Contacts for Ion-Selective Electrodes. Electronic Supplementary Information (ESI) Available: Synthetic and Spectroscopic Data for 1 and 2 Is Available from the RSC Web Site: *Chem. Commun.* **2000**, *0* (5), 339–340.
- (16) Fibbioli, M.; Morf, W. E.; Badertscher, M.; Rooij de, N. F.; Pretsch, E. Potential Drifts of Solid-Contacted Ion-Selective Electrodes Due to Zero-Current Ion Fluxes Through the Sensor Membrane. *Electroanalysis* **2000**, *12* (16), 1286–1292.
- (17) Wenzel, M. J.; Mensah-Brown, A.; Josse, F.; Yaz, E. E. Online Drift Compensation for Chemical Sensors Using Estimation Theory. *IEEE Sens. J.* **2011**, *11* (1), 225–232.
- (18) Cooper, J. S.; Myers, M.; Chow, E.; Hubble, L. J.; Cairney, J. M.; Pejcic, B.; Müller, K.-H.; Wieczorek, L.; Raguse, B. Performance of Graphene, Carbon Nanotube, and Gold Nanoparticle Chemiresistor Sensors for the Detection of Petroleum Hydrocarbons in Water. J. Nanopart. Res. 2014, 16 (1), 2173.
- (19) Isaad, J.; Salaün, F. Functionalized Poly (Vinyl Alcohol) Polymer as Chemodosimeter Material for the Colorimetric Sensing of Cyanide in Pure Water. Sens. Actuators, B 2011, 157 (1), 26–33.
- (20) Bittencourt, C.; Llobet, E.; Ivanov, P.; Correig, X.; Vilanova, X.; Brezmes, J.; Hubalek, J.; Malysz, K.; Pireaux, J. J.; Calderer, J. Influence of the Doping Method on the Sensitivity of Pt-Doped Screen-Printed SnO2 Sensors. *Sens. Actuators*, B **2004**, 97 (1), 67–73.
- (21) Cantalini, C.; Faccio, M.; Ferri, G.; Pelino, M. The Influece of Water Vapour on Carbon Monoxide Sensitivity of α -Fe2O3Microporous Ceramic Sensors. *Sens. Actuators, B* **1994**, *19* (1), 437–442.
- (22) Li, Y.-T.; Qu, L.-L.; Li, D.-W.; Song, Q.-X.; Fathi, F.; Long, Y.-T. Rapid and Sensitive In-Situ Detection of Polar Antibiotics in Water Using a Disposable Ag-Graphene Sensor Based on Electrophoretic Preconcentration and Surface-Enhanced Raman Spectroscopy. *Biosens. Bioelectron.* **2013**, 43, 94–100.
- (23) Mahar, B.; Laslau, C.; Yip, R.; Sun, Y. Development of Carbon Nanotube-Based Sensors—A Review. *IEEE Sens. J.* **2007**, *7* (2), 266–284.
- (24) Aslam, M.; Ahmad, R.; Kim, J. Recent Developments in Biofouling Control in Membrane Bioreactors for Domestic Wastewater Treatment. *Sep. Purif. Technol.* **2018**, 206, 297–315.
- (25) Chang, Z.; Zhu, Y.; Zhang, L.; Du, S. Measurement Experiment and Mathematical Model of Nitrate Ion Selective Electrode. *In 2013 Third International Conference on Instrumentation, Measurement, Computer, Communication and Control* **2013**, 48–52.
- (26) Carmel, L.; Levy, S.; Lancet, D.; Harel, D. A Feature Extraction Method for Chemical Sensors in Electronic Noses. *Sens. Actuators, B* **2003**, 93 (1), 67–76.
- (27) Sothivelr, K.; Bender, F.; Josse, F.; Yaz, E. E.; Ricco, A. J.; Mohler, R. E. Online Chemical Sensor Signal Processing Using Estimation Theory: Quantification of Binary Mixtures of Organic Compounds in the Presence of Linear Baseline Drift and Outliers. *IEEE Sens. J.* 2016, 16 (3), 750–761.
- (28) Han, T.; Mattinen, U.; Bobacka, J. Improving the Sensitivity of Solid-Contact Ion-Selective Electrodes by Using Coulometric Signal Transduction. *ACS Sens.* **2019**, *4* (4), 900–906.
- (29) Vergara, A.; Vembu, S.; Ayhan, T.; Ryan, M. A.; Homer, M. L.; Huerta, R. Chemical Gas Sensor Drift Compensation Using Classifier Ensembles. *Sens. Actuators, B* **2012**, *166–167*, 320–329.
- (30) Wang, H.; Fan, W.; Yu, P. S.; Han, J. Mining Concept-Drifting Data Streams Using Ensemble Classifiers. In *Proceedings of the Ninth ACM SIGKDD International Conference on Knowledge Discovery and Data Mining*; KDD '03; Association for Computing Machinery: Washington, D.C., 2003; pp 226–235. DOI: 10.1145/956750.956778.
- (31) Liikanen, A.; Martikainen, P. J. Effect of Ammonium and Oxygen on Methane and Nitrous Oxide Fluxes across Sediment-Water Interface in a Eutrophic Lake. *Chemosphere* **2003**, *52* (8), 1287–1293.
- (32) Bobacka, J. Conducting Polymer-Based Solid-State Ion-Selective Electrodes. *Electroanalysis* **2006**, *18* (1), 7–18.

- (33) Wang, J. Analytical Electrochemistry, 3. ed.; Wiley-VCH: Hoboken, NJ, 2006. DOI: 10.1002/0471790303.
- (34) Zoski, C. G.; Leddy, Johna.; Bard, A. J.; Faulkner, L. R. Student Solutions Manual to a Accompany Electrochemical Methods Fundamentals and Applications, 2nd ed.; Allen, J. B., Larry, R. F., Eds.; Wiley: New York, 2002;
- (35) Huang, Y.; Wang, T.; Xu, Z.; Hughes, E.; Qian, F.; Lee, M.; Fan, Y.; Lei, Y.; Brückner, C.; Li, B. Real-Time in Situ Monitoring of Nitrogen Dynamics in Wastewater Treatment Processes Using Wireless, Solid-State, and Ion-Selective Membrane Sensors. *Environ. Sci. Technol.* **2019**, 53 (6), 3140–3148.
- (36) Wang, T.; Xu, Z.; Huang, Y.; Dai, Z.; Wang, X.; Lee, M.; Bagtzoglou, C.; Brückner, C.; Lei, Y.; Li, B. Real-Time in Situ Auto-Correction of K+ Interference for Continuous and Long-Term NH4+ Monitoring in Wastewater Using Solid-State Ion Selective Membrane (S-ISM) Sensor Assembly. *Environ. Res.* 2020, 189, 109891.
- (37) Ahmed, F.; Lalia, B. S.; Kochkodan, V.; Hilal, N.; Hashaikeh, R. Electrically Conductive Polymeric Membranes for Fouling Prevention and Detection: A Review. *Desalination* **2016**, 391, 1–15.
- (38) Oztekin, E.; Altin, S. Wastewater Treatment by Electrodialysis System and Fouling Problems. *The Online Journal of Science and Technology.* 2016, 6 (1), 9.
- (39) Tamai, Y.; Matsunaga, T.; Horiuchi, K. Surface Energy Analysis of Several Organic Polymers: Comparison of the Two-Liquid-Contact-Angle Method with the One-Liquid-Contact-Angle Method. *J. Colloid Interface Sci.* 1977, 60 (1), 112–116.
- (40) Liu, B.; Chen, C.; Zhang, W.; Crittenden, J.; Chen, Y. Low-Cost Antifouling PVC Ultrafiltration Membrane Fabrication with Pluronic F 127: Effect of Additives on Properties and Performance. *Desalination* **2012**, 307, 26–33.
- (41) Hou, X.; Deem, P. T.; Choy, K.-L. Hydrophobicity Study of Polytetrafluoroethylene Nanocomposite Films. *Thin Solid Films* **2012**, 520 (15), 4916–4920.
- (42) Capodaglio, A. G. Integrated, Decentralized Wastewater Management for Resource Recovery in Rural and Peri-Urban Areas. Resources 2017, 6 (2), 22.
- (43) USEPA, O. Clean Water Act (CWA) Compliance Monitoring https://www.epa.gov/compliance/clean-water-act-cwa-compliance-monitoring (accessed 2020/9/10).
- (44) Delauney, L.; Compere, C.; Lehaitre, M. Biofouling Protection for Marine Environmental Sensors. *Ocean Sci.* **2010**, *6* (2), 503–511.
- (45) Bourgeois, W.; Romain, A.-C.; Nicolas, J.; M. Stuetz, R. The Use of Sensor Arrays for Environmental Monitoring: Interests and Limitations. *J. Environ. Monit.* **2003**, *5* (6), 852–860.
- (46) Oka, E. Long-Term Sensor Drift Found in Recovered Argo Profiling Floats. J. Oceanogr. 2005, 61 (4), 775–781.
- (47) Bell, S.; Dunand, F. A Comparison of Amperometric and Optical Dissolved Oxygen Sensors in Power and Industrial Water Applications at http://Low/paper/A-Comparison-of-Amperometric-and-Optical-Dissolved-Bell-Dunand/85d6b56d1f0c3e3e800cb41d7e0f3f34b520931f (accessed 2020/9/15).
- (48) Helder, D.; Anderson, C.; Beckett, K.; Houborg, R.; Zuleta, I.; Boccia, V.; Clerc, S.; Kuester, M.; Markham, B.; Pagnutti, M. Observations and Recommendations for Coordinated Calibration Activities of Government and Commercial Optical Satellite Systems. *Remote Sens.* 2020, 12 (15), 2468.
- (49) Horsburgh, J. S.; Tarboton, D. G.; Maidment, D. R.; Zaslavsky, I. Components of an Environmental Observatory Information System. *Comput. Geosci.* **2011**, *37* (2), 207–218.
- (50) Guidelines and standard procedures for continuous water-quality monitors: Station operation, record computation, and data reporting https://pubs.er.usgs.gov/publication/tm1D3 (accessed 2020/9/15).
- (51) Adu-Manu, K. S.; Tapparello, C.; Heinzelman, W.; Katsriku, F. A.; Abdulai, J.-D. Water Quality Monitoring Using Wireless Sensor Networks: Current Trends and Future Research Directions. *ACM Trans. Sens. Netw.* **2017**, *13* (1), 4:1–4:41.

- (52) Romain, A. C.; Nicolas, J. Long Term Stability of Metal Oxide-Based Gas Sensors for e-Nose Environmental Applications: An Overview. Sens. Actuators, B **2010**, 146 (2), 502–506.
- (53) Shaughnessy, A. R.; Prener, C. G.; Hasenmueller, E. A. An R Package for Correcting Continuous Water Quality Monitoring Data for Drift. *Environ. Monit. Assess.* **2019**, *191* (7), 445.
- (54) Gao, W.; Emaminejad, S.; Nyein, H. Y. Y.; Challa, S.; Chen, K.; Peck, A.; Fahad, H. M.; Ota, H.; Shiraki, H.; Kiriya, D.; Lien, D.-H.; Brooks, G. A.; Davis, R. W.; Javey, A. Fully Integrated Wearable Sensor Arrays for Multiplexed in Situ Perspiration Analysis. *Nature* **2016**, *529* (7587), 509–514.
- (55) Maleknejad, K.; Aghazadeh, N. Numerical Solution of Volterra Integral Equations of the Second Kind with Convolution Kernel by Using Taylor-Series Expansion Method. *Appl. Math. Comput.* **2005**, *161* (3), 915–922.
- (56) Du, J.; Huo, Q. A Feature Compensation Approach Using High-Order Vector Taylor Series Approximation of an Explicit Distortion Model for Noisy Speech Recognition. *IEEE Trans. Audio Speech Lang. Process.* **2011**, *19* (8), 2285–2293.
- (57) Lee, S. H.; Rasaiah, J. C. Molecular Dynamics Simulation of Ion Mobility. 2. Alkali Metal and Halide Ions Using the SPC/E Model for Water at 25 °C. *J. Phys. Chem.* **1996**, *100* (4), 1420–1425.
- (58) Morf, W. E.; Badertscher, M.; Zwickl, T.; Reichmuth, P.; de Rooij, N. F.; Pretsch, E. Calculated Effects of Membrane Transport on the Long-Term Response Behavior of Polymeric Membrane Ion-Selective Electrodes. *J. Phys. Chem. B* **2000**, *104* (34), 8201–8209.
- (59) Werner, W. Polynomial Interpolation: Lagrange versus Newton. *Math. Comput.* **1984**, *43* (167), 205–217.
- (60) Scott, A. J.; Knott, M. A Cluster Analysis Method for Grouping Means in the Analysis of Variance. *Biometrics* **1974**, *30* (3), 507–512.
- (61) Aggarwal, C. C. Cluster Analysis. In *Data Mining: The Textbook*; Aggarwal, C. C., Ed.; Springer International Publishing: Cham, 2015; pp 153–204. DOI: 10.1007/978-3-319-14142-8 6.
- (62) M?ller, T.; Machiraju, R.; Mueller, K.; Yagel, R. Classification and Local Error Estimation of Interpolation and Derivative Filters for Volume Rendering. *In Proceedings of 1996 Symposium on Volume Visualization* **1996**, 71–78.
- (63) M?ller, T.; Machiraju, R.; Mueller, K.; Yagel, R. Evaluation and Design of Filters Using a Taylor Series Expansion. *IEEE Trans. Vis. Comput. Graph.* 1997, 3 (2), 184–199.
- (64) Normal Distribution I https://www.encyclopedia.com/science-and-technology/mathematics/mathematics/normal-distribution#3 (accessed 2020/5/6).
- (65) Parzen, E. On Estimation of a Probability Density Function and Mode. *Ann. Math. Stat.* **1962**, 33 (3), 1065–1076.
- (66) Rosenblatt, M. Remarks on Some Nonparametric Estimates of a Density Function. *Ann. Math. Stat.* **1956**, 27 (3), 832–837.
- (67) Westfall, P. H. Kurtosis as Peakedness, 1905–2014. R.I.P. Am. Stat. 2014, 68 (3), 191–195.
- (68) Ohki, M.; Zervakis, M. E.; Venetsanopoulos, A. N. 3-D Digital Filters. In Control and Dynamic Systems: Multidimensional Systems: Signal Processing and Modeling Techniques; Leondes, C. T., Ed.; Academic Press, 1995; Vol. 69, pp 49–88. DOI: 10.1016/S0090-5267(05)80038-6.
- (69) Park, S. S.; Altintas, Y. Dynamic Compensation of Spindle Integrated Force Sensors With Kalman Filter. *J. Dyn. Syst., Meas., Control* **2004**, 126 (3), 443–452.
- (70) Lee, H.-J.; Jung, S. Gyro Sensor Drift Compensation by Kalman Filter to Control a Mobile Inverted Pendulum Robot System. *In 2009 IEEE International Conference on Industrial Technology* **2009**, 1–6.
- (71) Zimmerschied, R.; Isermann, R. Nonlinear Time Constant Estimation and Dynamic Compensation of Temperature Sensors. *Control Eng. Pract.* **2010**, *18* (3), 300–310.
- (72) Wang, L.; Yang, D.; Lamb, D.; Chen, Z.; Lesniewski, P. J.; Megharaj, M.; Naidu, R. Application of Mathematical Models and Genetic Algorithm to Simulate the Response Characteristics of an Ion Selective Electrode Array for System Recalibration. *Chemom. Intell. Lab. Syst.* 2015, 144, 24–30.

- (73) Wang, L.; Yang, D.; Fang, C.; Chen, Z.; Lesniewski, P. J.; Mallavarapu, M.; Naidu, R. Application of Neural Networks with Novel Independent Component Analysis Methodologies to a Prussian Blue Modified Glassy Carbon Electrode Array. *Talanta* **2015**, *131*, 395–403.
- (74) Nuñez, L.; Cetó, X.; Pividori, M. I.; Zanoni, M. V. B.; del Valle, M. Development and Application of an Electronic Tongue for Detection and Monitoring of Nitrate, Nitrite and Ammonium Levels in Waters. *Microchem. J.* **2013**, *110*, 273–279.
- (75) Gutiérrez, M.; Alegret, S.; Cáceres, R.; Casadesús, J.; Marfa, O.; del Valle, M. Application of a Potentiometric Electronic Tongue to Fertigation Strategy in Greenhouse Cultivation. *Comput. Electron. Agric.* **2007**, *57* (1), 12–22.
- (76) Lu, R.; Sheng, G.; Li, W.; Yu, H.; Raichlin, Y.; Katzir, A.; Mizaikoff, B. IR-ATR Chemical Sensors Based on Planar Silver Halide Waveguides Coated with an Ethylene/Propylene Copolymer for Detection of Multiple Organic Contaminants in Water. *Angew. Chem., Int. Ed.* **2013**, *52* (8), 2265–2268.
- (77) Archer, M.; Christophersen, M.; Fauchet, P. M. Electrical Porous Silicon Chemical Sensor for Detection of Organic Solvents. *Sens. Actuators, B* **2005**, *106* (1), 347–357.
- (78) Khorshid, A. F.; Amin, R. R.; Issa, Y. M. Fabrication of a Novel Highly Selective and Sensitive Nano-Molar Cu(I), Cu(II) Membrane Sensors Based on Thiosemicarbazide and Acetaldehydethiosemicarbazone Copper Complexes https://www.semanticscholar.org/paper/Fabrication-of-a-Novel-Highly-Selective-and-Cu(I)%2C-Khorshid-Amin/2bba6002aad8e55964a7de8e92e86b7d5d2ee299 (accessed 2020/5/14).
- (79) Mohamed, G. G.; Ali, T. A.; El-Shahat, M. F.; Al-Sabagh, A. M.; Migahed, M. A.; Khaled, E. Potentiometric Determination of Cetylpyridinium Chloride Using a New Type of Screen-Printed Ion Selective Electrodes. *Anal. Chim. Acta* **2010**, *673* (1), 79–87.
- (80) De Marco, R.; Clarke, G.; Pejcic, B. Ion-Selective Electrode Potentiometry in Environmental Analysis. *Electroanalysis* **2007**, *19* (19–20), 1987–2001.